International Journal of Surgery Open 16 (2019) 22–28

Contents lists available at ScienceDirect

International Journal of Surgery Open

journal homepage: www.elsevier.com/locate/ijso

Research Paper

Pathway and workspace study of Endonasal Endoscopic Transsphenoidal (EET) approach in 80 cadavers

Sorayouth Chumnanvej [a], Suwiphat Chalongwongse [b], Branesh M. Pillai [b], Jackrit Suthakorn [b, *]

[a] Neurosurgery Division, Department of Surgery, Faculty of Medicine Ramathibodi Hospital, Mahidol University, Bangkok, Thailand
[b] Center for Biomedical and Robotics Technology (BART LAB), Department of Biomedical Engineering, Faculty of Engineering, Mahidol University, Salaya, Thailand

ARTICLE INFO

Article history:
Received 7 September 2018
Received in revised form
12 December 2018
Accepted 13 December 2018
Available online 17 December 2018

Keywords:
EETS pathway
Surgical workspace
Intrasellar lesions
Robotic surgery

ABSTRACT

Background: The Endonasal Endoscopic Transsphenoidal Surgery (EETS) is used to remove the sellar lesion. Because of the unique location of the lesion, a subtle deviation of tools may result in severe complications. The better coordination between workspace and working environment is vital. The aim of this study is to determine the pathways and workspace utilized in EETS. In addition, this result will be used to develop the robotic assisted technology model further.
Methods: Pathway and workspace details were studied in 80 soft cadavers and dissections were performed in a stepwise manner to simulate EETS. The optical tracking system was used to collect data. MATLAB programming was applied to analyze workspace and pathway. The descriptive data analysis was presented as percentage, mean, and standard deviation.
Results: The amplitude of P2S vectors or the length of the EETS workspace was around 70–75 mm. EETS workspace was found to be a cylindrical shape, narrow diameter in the middle with an average volume of 15.97 cm^3, the average length of 53.9 mm and average widest width of 19.08 mm.
Conclusion: This study presents characteristics of EETS pathway and workspace. Detailed knowledge of the EETS pathway and workspace will facilitate understanding for further robotic research.

1. Introduction

The Endonasal Endoscopic Transsphenoidal Surgery (EETS) has been a significant advancement in the diagnosis and treatment of interstellar lesions [16,26]. The EETS procedure provides exceptional exposure to the essential components of both the intrasellar lesions and the neighboring structures by offering a temporal and spatial surgical manipulation [9,27]. The EETS procedure can do so by providing a well-controlled surgical manipulation [10,17–19,38]. According to previous reports, EETS has the potential to replace the traditional microscopic skull base surgical procedures by introducing more precise visualization and minimal invasiveness [2,3,13,22,23].

The EET procedure has been recently developed and is carried out under the supervision of a skillful surgeon. This procedure works on the principle of two procedures i.e. access to sphenoid and tumor eradication [1,20]. During sphenoid sinus approaching process the major limitation is the lack of anatomical landmark inside nasal cavity [4,5,42]. Additionally, this procedure is time consuming and it takes more than an hour to conduct the surgery. Along with that there are chances of mucosal injury during the procedure due to slight tremor or deflection [8,12,41]. In case of the second principle the precision and accuracy of the tool is the key factor. It is basically the keen movement of the surgical tool that aids in tumor removal. This is lengthy procedure and may take 2–4 h. This procedure is conducted inside the brain, hence, requires extreme precision to avoid postoperative complications as shown in Fig. 1. The research illustrates (26.9%) of the patients experience postoperative [6,7,21].

This study is designed with a keen focus on the principles of workspace and pathway of EET procedure. The EET experiments were conducted on fresh 80 cadavers and the data is gathered based on the movement of the surgical tools. The analysis of the data is based on three parameters: motion of the surgical tool, shape and the dimension of the workspace. This study will aid in minimizing the time and the damage to mucosa of the nose. Conventional EET surgical procedures have tools with wider dimensions and to tackle the multiple tools in a narrow nasal passage becomes difficult

* Corresponding author.
E-mail addresses: sorayouth.chu@mahidol.ac.th (S. Chumnanvej), suwipat@bartlab.org (S. Chalongwongse), branesh@bartlab.org (B.M. Pillai), jackrit.sut@mahidol.ac.th (J. Suthakorn).

https://doi.org/10.1016/j.ijso.2018.12.002
2405-8572/

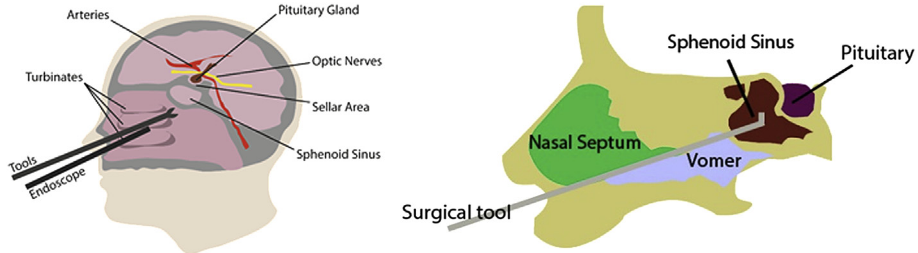

Fig. 1. Pituitary gland on head anatomy.

[14,15,40,43]. Therefore, EET robotic surgeries have yet not been validated and established for trans-nasal surgeries. The study under discussion has accomplished the fluoroscopic images for pre- and intra-operations. The robot guided EET system will ensure the safety of the patient and will aid in minimization of the technical obstacles in order to reach the target area of sphenoid sinus. In addition to this, will assist the surgeon by providing medical images and single time insertion will take place reducing the risk of damaging the mucosa due to multiple insertions.

The most important aspect of this surgical procedure is that it needs hour-long precise and detailed attention to reach to sphenoid sinus base area. Any minor mistake may lead to a fatal accident [24,25,30]. To address these issues, we did in-depth research on EETS procedure and pathways to guide and assist neurosurgeons. In addition, it is imperative to understand the surgical anatomy and potential anatomical variations of the intrasellar lesions before the practice of the EETS, especially when cadaveric dissections are involved. In this present work, we have executed bi-nasal endoscopic transsphenoidal surgery to evaluate the surgical pathway and workspace for the robot-assisted surgical design as shown in Fig. 2. In this context, we assessed the path of exposure and the characterized the workspace in detail by evaluating the volume, diameter, and length of the endonasal corridor.

This research countering the limitations associated with EET procedures. The focal area of this study is to conduct the surgery in lesser time with ultra-precision and fineness to hit the target. A robot based system is being introduced in this study where the primary pathway (nasal cavity to sphenoid sinus) to pituitary tumor will be performed by the surgeon but under the guidance of robot. A surgeon will perform the surgery that will be assisted by the robot. Robot will guide the receptacle in terms of its trajectory that will further lead to the provision of the precise passage for the endoscope or the surgical tool to reach the target. As afore mentioned, it is a lengthy procedure, an insignificant turbulence or deflection at the part of surgeon may lead to damage. Maintenance of a stable and steady trajectory is the key and this will be provided by the Robot guided system. Robot guided receptacle will mine the information through the images provided by fluoroscopy. These fluoroscopic images will be transferred to software that will guide the receptacle to alien its position. This will provide the surgeon a stable and precise pathway to reach the target with its surgical tool. Moreover, the route can be examined via connected computer systems. This study will aid in reducing the risk factors and the limitations associated with the conventional EETS system.

2. Material and method

Bi-nasal endoscopic transsphenoid surgery was carried out on 80 soft adult cadavers without any prior history of head trauma or craniofacial surgery. The cadavers were dissected following the initial autopsy examination and approval of the Department of Anatomy, Faculty of Science, Mahidol University. EETS to the intrasellar region was performed in a stepwise manner as discussed separately on protocol section below by the first author (SC). The variations in the bone and the neurovascular structures along the surgical path were noted down recorded and surgically important anatomic measurements were well documented. In this study, two outcome measures were considered for further robot-assisted surgical design; (1) pathway of exposure; (2) the workspace. In the later, we analyzed the volume, diameter and length of the endonasal corridor.

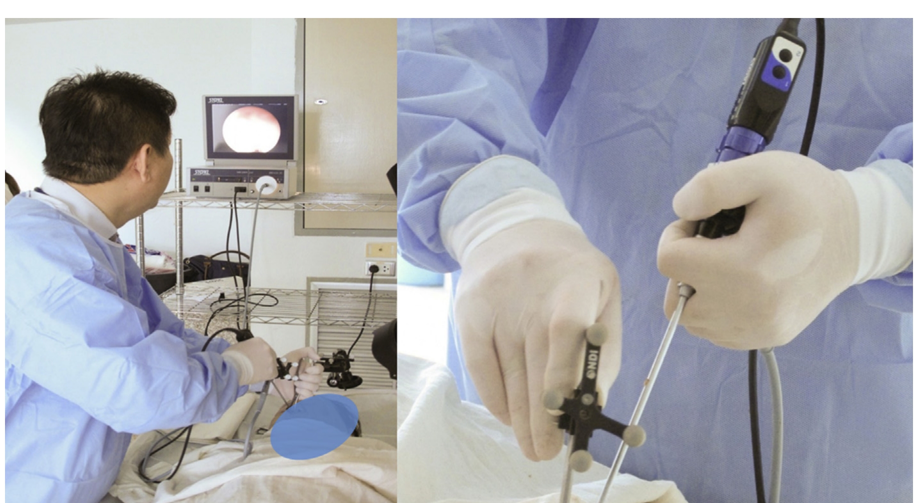

Fig. 2. Conventional bi-nasal endoscopic transsphenoidal procedures.

The optical tracking system (OTS, Polaris Vicra[R], Northern Digital Inc.) was used to detect the position and the orientation of all the EETS instruments including endoscope, dissectors and suction via infrared ray. The OTS has two major components; (1) the tracker and (2) the passive marker. While the tracker (or the NDI[R] camera) was used to generate the infrared ray, the passive marker was used to reflect the material. The distance between the tracker and the passive marker were computed by calculating the differences of wavelength between the rays generated from these two different sources to measure the position and orientation of the EETS instruments during the surgical procedure. Two sets of passive markers were attached to the surgical instruments and cadaveric head to detect the position and orientation of the surgical instruments and cadaver's head. Six different parameters were considered to represent position and orientation of the marker on the camera; 3 parameters for positions of XYZ coordinates and 3 parameters for orientation around XYZ coordinates and the final OTS data was saved as.csv files.

The target of this present study is the sphenoid sinus which is for the robot to reach. After the robot reached the target, the neurosurgeon will do the operation where the sellar area is the aim of the operation. The main objective is the robotic design and the robot will be controlled to reach sphenoid sinus. The neurosurgeon will identify and remove the lesion at the sellar area which the pituitary tumor is there. The boundary area is the sellar area where the neurosurgeon can identify safely to remove pituitary tumor. The experiments were carried out in the following step-wise procedure while executing the EET surgery on all the cadavers.

2.1. The nostril-nasal cavity pathway

- The patient was positioned in a supine posture with fixed head and the nasal cavities were prepped.
- Manually, the endoscope, followed by the dissectors was inserted through the nasal cavity and the sphenoid sinus base was identified.

2.2. The sphenoid sinus-sellar floor pathway

- Once the sphenoid sinus base was defined, the eggshell like bone of the sphenoid sinus base was exposed and trimmed out to reach out the sphenoid sinus.
- It was followed by the identification of the sellar floor of sella turcica, which is a thin and fragile bone. The dura mater, boundary area of the tumor and bilateral great vessels were confined to this region.
- The gross total tumor removal (GTR) was performed, and the incision on skull base is closed by either by the pedicular soft tissue or by the fat or by the cartilage or by the synthetic material to prevent cerebrospinal fluid (CSF) leakage.

The step-wise surgical procedure is presented in Fig. 3. Briefly, Tool-tip position and orientation was defined by calibrating the optical marker tool-tip. The marker was then set at the vertex of the cadaver head and the optical tracking (NDI[R]) was set up accordingly. The tool was then introduced to the sphenoid sinus base through the columella.

Since the differences of the distance and direction of the tool in each time of the operation was variable, the collected data could not be compared. However, to make it comparable, we applied homogeneous transformation matrix on the same reference background.

In this bi-nasal approach; we performed the experiment both on left side and right side and on average each experiment took 3–5 min. We collected about 700 points from each nasal cavity and applied the homogeneous transformation matrix equation to analyze the data. The equation is presented as below.

$$^{NDI}_{point_i}H = {}^{NDI}_{Columella}H * {}^{Columella}_{point_i}H$$

$$^{Columella}_{point_i}H = {}^{NDI}_{Columella}H^{-1} * {}^{NDI}_{point_i}H$$

Using the above equations, it is calculated the inverse matrix of transformation matrix from origin frame to cadaver's head and multiplied the value with transformation matrix from origin frame to surgical tool. As a result, it is possible to compare experimental data to each other.

We considered shape, dimension and volume factors to analyze the EETS workspace data. While the dimension of EETS workspace was considered from maximum boundary, the length of the workspace is defined from the columella to the sphenoid sinus base. We considered the largest cross sections area of the workspace to calculate the diameter of the shape. From the raw cloud point data we calculated the volume of the workspace by applying the Delaunay triangulation method, which was created from 3 neighbor points of the data without any background contamination. Then the calculated area of all the triangular points were used to estimate the total volume of the workspace directly by adding all the individual areas (Fig. 4).

3. Results

3.1. EETS pathway analysis

The EETS pathway was analyzed by estimating the real time positions and orientations of the surgical instruments during the operation and was considered from depth of surgical instruments on EETS workspace. During this procedure, we determined the character of each data point by determining a P2S vector for each data point, which is nothing but a vector from the columella to the sphenoid sinus base. This was followed by the computation of X-Z plane from each P2S vector by utilizing the homogeneous transformation matrix. By doing so, once the P2S vector was moved to X-Z plane, again the vector was moved to Z-axis by applying same transformation matrix. Finally, we applied the transformation matrix to all data point to define the end homogeneity of the transformation of P2S vector to Z-axis.

For the normalization of length: we transferred all the points and the P2S vectors to the Z-axis and normalized the amplitude of all P2S vectors. We found the amplitude of P2S vectors (length of EETS workspace) to be around 70–75 mm, whose value was changed to 80 mm after normalization. Once the values were normalized, by adapting the window function, the cloud points of surgical instruments position are sliced into small values. The window with 5 mm wide was run on the P2S vector with a step of 2 mm value.

Next, we calculated the Probability Density Function (PDF) of XY positions a 2D plane in cross section view, which simply represents the frequency used position at each depth of surgical tool tip (Fig. 5). Each cross section had a dimension of 0.5 $\times$ 0.5 grid and different colors are assigned to distinguish the number of surgical tool tip positions on each grid. In Fig. 5 dark blue shaded area represents small frequency of position and light blue shaded area represents the most frequency of position.

The overall orientation of the surgical tool tip of each 2 mm step depth from columella to sphenoid sinus base derived from the PDF values of orientation; the PDF values obtained from the 3 to 5 most frequently used positions (Fig. 6).

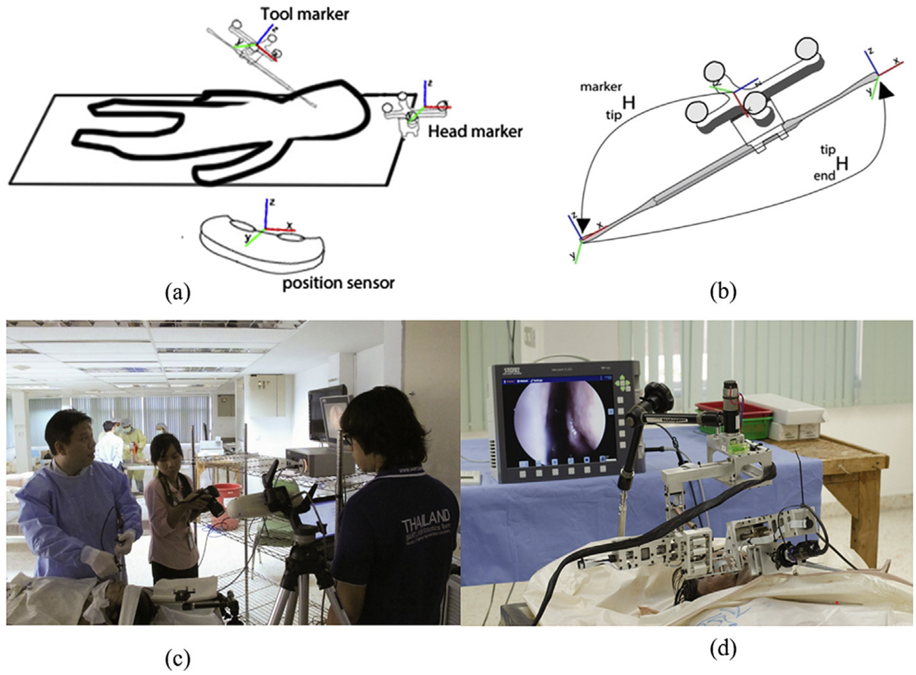

Fig. 3. Surgical methodology describing the tool-tip position and orientation during a cadaver surgery. (a) System Overview (b) tool coordinate transformation (c) Conventional EETS bi-nasal approach (d) EETS Robotic approach.

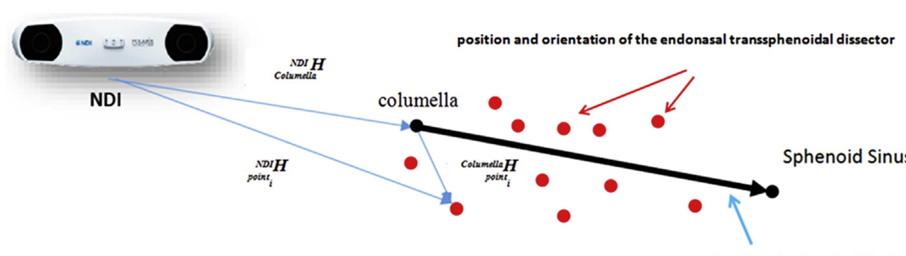

Fig. 4. Homogenous transformation model from the optical tracking system, columella and sphenoid sinus base.

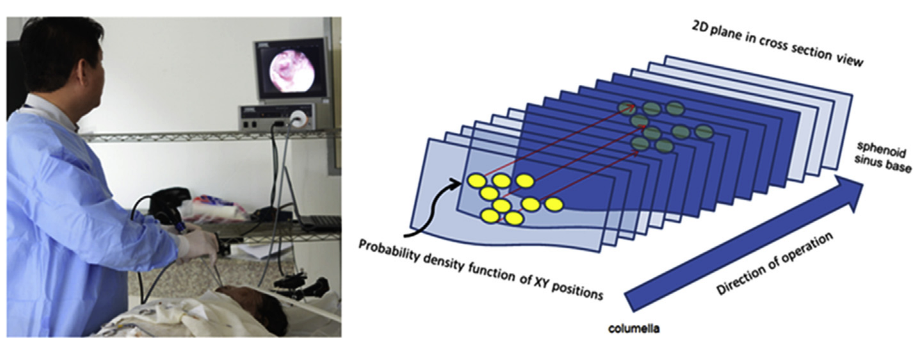

Fig. 5. EETS pathways in 2D plane cross-section view. PDF of XY positions (yellow circle) are random at the most dense area where the dissector was passed through the columella to reach sphenoid sinus base. Red arrows represent the most frequent position of each slice, and the orientation of the arrows present orientation of surgical tool tip. Size of the arrows show number of frequency of each position.

The different parameters of the EETS workspace between the experiments were analyzed. The maximum, minimum, average and standard deviation values are presented in Table 1.

Finding the statistical significance in any of the parameters between the left and right nostril is a complex and failure part. This suggests a conserved but subtle anatomical variation between the left and right nostrils.

4. Discussion

The shortest and workable pathway to the intrasellar region is the transsphenoidal midline route [10,11]. This way provides not only an affordable workspace but also offers a low mortality rate [28,29,32,34,36]. While the introduction of the endoscope to the intrasellar region has been a challenging for past several decades,

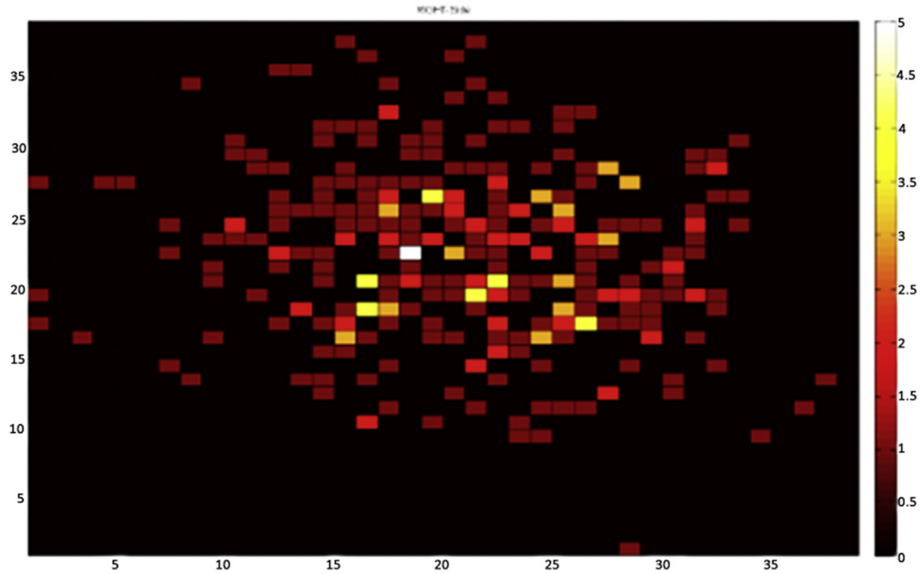

Fig. 6. The Probability Density Function (PDF) of the values of each slice. The frequency position is color coded on the right hand side heat map bar.

recent advancements on these shortcomings have made it possible to deal with skull base surgeries [26,27]. To this end, establishing EETS to the intrasellar region has been the first revolutionary step in the field and the endoscopic skull base surgeries [9,13,39].

However, even though one of the hurdles has been taken care of with the advancement of technology, obtaining specimens in these types of studies became a major limiting factor and hard to achieve [17,18]. This issue can be addressed partially by conducting experiments on the limited number of specimens, it may results in significant variation between trials because of insufficient specimen numbers. Additionally, we brought to the reader's attention as we found it significant differences in few our results due to the lack of sample number. Present study determines the characteristics and movement of the surgical tool during EETS procedures. The analysis of the ideal EETS workspace and pathway, was suitable for the robot-assisted surgical design.

This research proposes a methods to determine the pathways and workspace utilized in the EETS approach with an ultimate goal to guide and assist neurosurgeons during EETS procedure. Besides, it is crucial for the neurosurgeons be aware of the intrasellar anatomical variations along the surgical workspace and the target region from the endoscopic view to execute a standard EETS in the intrasellar region. For example, it is hard to identify the sphenoid sinus base. From the research investigation [31,33,35,37] it is evident that at least in 75% cases, most surgeons detect sphenoid sinus base about 10–12 mm superior to the posterior nasal aperture. From our workspace correlation, we detected a linear relationship between the Sphenoid Sinus and Nostril spatial distribution as shown in the (Fig. 7).

Out of several different possible shape types, we found the shape of the workspace in our study is cylindrical with a narrow diameter at the middle (Fig. 8). Even though the workspace looked narrower, we found a significant safe distance between the two internal carotid arteries (ICA) to open the intrasellar floor and expose the pituitary gland. Also, we were able to locate the diaphragma sellae in all 80 specimens following total hypophysectomy.

These factors are important as the inability to recognize important anatomical structures along the surgical pathway may intervene with the endoscopic manipulations and prolong the surgical time. However, with our unique approach of determining the pathways and workspace utilized during the EET, we were able to overcome these issues. In our opinion, these factors are vital in determining the overall success of any endoscopic skull base surgery, especially if performed without image guidance.

This study summarizes the variations in nasal, sphenoidal and intrasellar phases of the EETS procedures and provides a better model to overcome the associated issues. The outcome of the work suggests having a detailed knowledge of the fundamental

Table 1
EETS parameters between the experiments (left and right nostril).

Parameter	Statistical data			
	Minimum	Maximum	Average	Standard deviation
Volume (cm^3)				
L	7.73	26.86	16.16	5.92
R	5.61	28.87	15.78	6.20
All	5.61	28.87	15.97	6.02
Diameter (mm)				
L	14.28	25.89	13.32	3.23
R	13.28	27.26	18.84	3.46
All	13.28	27.26	19.08	3.32
Length (mm)				
L	36.01	70.46	53.55	8.39
R	40.5	70	54.24	5.91
All	36.01	70.46	53.9	7.2

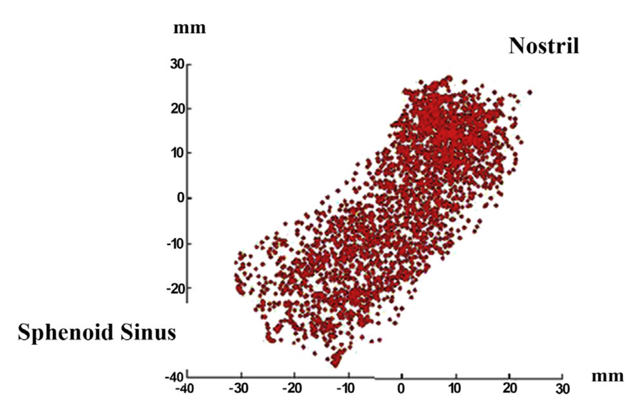

Fig. 7. Workspace of EETS showing the spatial.

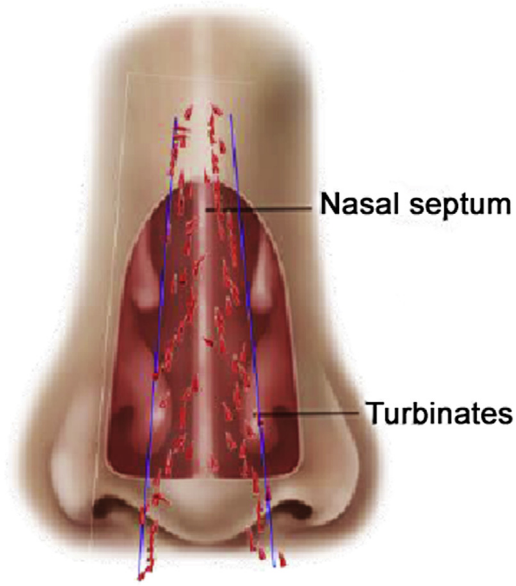

Fig. 8. Pathway model in bi-nasal cavities.

anatomical relationships in the context of the endoscopic dissections in a large and cumulative number of specimens. Results from our work will facilitate endoscopic surgical procedures and decrease the rate of surgical complications.

Ethical approval

Cadaveric based experiments were conducted and an Ethical approval statement is enclosed as an electronic supplementary material.

Funding

This research has been funded by the Computer-Integrated Intelligent Medical System Project under the National Research University Grant through Mahidol University. Another fund resource is Commercializing Development of a Virtual Reality Based Surgical Robotic Training System with Haptic Force Feedback Project, Granted by Thailand Center of Excellence for Life Sciences (TCELS), (Grant Number: TC 20/60).

Author contribution

All authors have discussed and commented on the manuscript at all stages. More specifically, Sorayouth Chumnanvej, Suwiphat Chalongwongse and Branesh M. Pillai collected the related literature, conducted the analysis, and completed the draft writing under the supervision of Jackrit Suthakorn, who has also contributed to the revision of the paper structure and the presentation style, as well as the proofreading of the paper.

Conflict of interest statement

The authors of this paper have no conflicts of interest or financialties to disclose.

Guarantor

Jackrit Suthakorn.

Research registration number

ID-11-55-10.

Acknowledgements

We would like to thank Ramathibodi Hospital staff and residents for their valuable knowledge and recommendations towards the development of this system. Another group we would like to thank are the BARTLAB members who presented us with knowledge in mechanical design, programming, and statistical analysis.

References

[1] Alfieri A, Jho H. Endoscopic endonasal cavernous sinus surgery: an anatomic study. Neurosurgery 2001;48:827–37.
[2] Alfieri A, Jho HD. Endoscopic endonasal approaches to the cavernous sinus: surgical approaches. Neurosurgery 2001;49:354–62.
[3] Al-Nashar IS, Carrau RL, Herrera A, Synderman CH. Endoscopic transnasal transpterygopalatine fossa approach to the lateral recess of the sphenoid sinus. Laryngoscope 2004;114:528–32.
[4] Aust MR, McCaffrey TV, Atkinson J. Transnasal endoscopic approach to the sella turcica. Am J Rhinol 1998;12:283–7.
[5] Badie B, Nguyen P, Preston J. Endoscopic-guided direct endonasal approach for pituitary surgery. Surg Neurol 2000;53:168–73.
[6] Barzilay Y, Liebergall M, Fridlander A, Knoller N. Miniature robotic guidance for spine surgery–introduction of a novel system and analysis of challenges encountered during the clinical development phase at two spine centres. Int J Med Robot 2006;2:146–53.
[7] Brandmeir NJ, Savaliya S, Rohatgi P, Sather M. The comparative accuracy of the ROSA stereotactic robot across a wide range of clinical applications and registration techniques. J Robot Surg 2018;12:157–63.
[8] Bolger WE. Endoscopic transpterygoid approach to the lateral sphenoid recess: surgical approach and clinical experience. Arch Otolaryngol Head Neck Surg 2005;133:20–6.
[9] Cappabianca P, Alfieri A, de Divitiis E. Endoscopic endonasal transsphenoidal approach to the sella: towards functional endoscopic pituitary surgery (FEPS). Minim Invasive Neurosurg 1998;41:66–73.
[10] Cappabianca P, Cavallo LM, Colao A, Del Basso De Caro M, Esposito F, Cirillo S, et al. Endoscopic endonasal transsphenoidal approach: outcome analysis of 100 consecutive procedures. Minim Invasive Neurosurg 2002;45:193–200.
[11] Cappabiancal P, Alfieri A, Colao A, Cavallo LM, Fusco M, Peca C, et al. Endoscopic endonasal transsphenoidal surgery in recurrent and residual pituitary adenomas: technical note. Minim Invasive Neurosurg 2000;43:38–43.
[12] Cappabianca P, Cavallo LM, Colao A, de Divitiis E. Surgical complications associated with the endoscopic endonasal transsphenoidal approach for pituitary adenomas. J Neurosurg 2002;97:293–8.
[13] Cappabianca P, de Divitiis E. Endoscopy and transsphenoidal surgery. Neurosurgery 2004;54:1043–50.
[14] Cappabianca P, Cavallo LM, Solari D, Stagno V, Esposito F, de Angelis M. Endoscopic endonasal surgery for pituitary adenomas. World Neurosurg 2014;82:S3–11.
[15] Cappabianca P, Cavallo LM, Solari D, Esposito F. Endoscopic endonasal transsphenoidal approach to pituitary adenomas. J Neurosurg 2015;122:473–4.
[16] Carrau RL, Jho HD, Ko Y. Transnasal trans-sphenoidal endoscopic surgery of the pituitary gland. Laryngoscope 1996;106:914–8.
[17] Catapano D, Sloffer CA, Frank G, Pasquini E, D'Angelo VA, Lanzino G. Comparison between the microscope and endoscope in the direct endonasal extended transsphenoidal approach: anatomical study. J Neurosurg 2006;104:419–25.
[18] Cavallo LM, Messina A, Cappabianca P, Esposito F, de Divitiis E, Gardner P, et al. Endoscopic endonasal surgery of the midline skull base: anatomical study and clinical considerations. Neurosurg Focus 2005;19:E2.
[19] Charalampaki P, Reisch R, Ayad A, Conrad J, Welschehold S, Perneczky A, et al. Endoscopic endonasal pituitary surgery: surgical and outcome analysis of 50 cases. J Clin Neurosci 2007;14:410–5.
[20] Christian E, Harris B, Wrobel B, Zada G. Endoscopic endonasal transsphenoidal surgery: implementation of an operative and perioperative checklist. Neurosurg Focus 2014;37:E1.
[21] Devito DP, Kaplan L, Dietl R, Pfeiffer M, Horne D, Silberstein B, et al. Clinical acceptance and accuracy assessment of spinal implants guided with SpineAssist surgical robot: retrospective study. Spine (Phila Pa 1976) 2010;35:2109–15.
[22] de Divitiis E, Cappabianca P, Cavallo LM. Endoscopic transsphenoidal approach: adaptability of the procedure to different sellar lesions. Neurosurgery 2002;51:699–707.
[23] de Divitiis E, Cappabianca P. Microscopic and endoscopic transsphenoidal surgery. Neurosurgery 2002;51:1527–30.
[24] Farrell CJ, Nyquist GG, Farag AA, Rosen MR, Evans JJ. Principles of pituitary surgery. Otolaryngol Clin North Am 2016;49:95–106.

[25] Gondim JA, Almeida JP, de Albuquerque LA, Gomes E, Schops M, Mota JI. Endoscopic endonasal transsphenoidal surgery in elderly patients with pituitary adenomas. J Neurosurg 2015;123:31–8.
[26] Jho HD, Carrau RL, Ko Y, Daly MA. Endoscopic pituitary surgery: an early experience. Surg Neurol 1997;47:213–23.
[27] Jho HD, Carrau RL. Endoscopic endonasal trans-sphenoidal surgery: experience with 50 patients. Neurosurg Focus 1996;1:1–6.
[28] Lang J. Clinical anatomy of the nose, nasal cavity and the paranasal sinuses. New York: Thieme; 1989.
[29] Laws ER, Kanter AS, Jane Jr JA, Dumont JS. Extended transsphenoidal approach. J Neurosurg 2005;102:825–8.
[30] Laws ER, Wong JM, Smith TR, de Los Reyes K, Aglio LS, Thorne AJ, et al. A checklist for endonasal transsphenoidal anterior skull base surgery. J Neurosurg 2016;124:1634–9.
[31] Mendelson ZS, Husain Q, Kanumuri VV, Eloy JA, Liu JK. Endoscopic transsphenoidal surgery of Rathke's cleft cyst. J Clin Neurosci 2015;22:149–54.
[32] Moreland DB, Diaz-Ordaz E, Czajka GA. Endoscopic endonasal hemisphenoidotomy for resection of pituitary lesions confined to the sella: report of 3 cases and technical note. Minim Invasive Neurosurg 2000;43:57–61.
[33] Oertel J, Gaab MR, Linsler S. The endoscopic endonasal transsphenoidal approach to sellar lesions allows a high radicality: the benefit of angled optics. Clin Neurol Neurosurg 2016;146:29–34.
[34] Perneczky A, Fries G. Endoscope-assisted brain surgery: part 1- evolution, basic concept, and current technique. Neurosurgery 1998;42:219–25.
[35] Pinar E, Yuceer N, Imre A, Guvenc G, Gundogan O. Endoscopic endonasal transsphenoidal surgery for pituitary adenomas. J Craniofac Surg 2015;26:201–5.
[36] Pirris SM, Pollack IF, Snyderman CH, Carrau RL, Spiro RM, Tyler-Kabara E, et al. Corridor surgery: the current paradigm for skull base surgery. Childs Nerv System 2007;23:377–84.
[37] Qureshi T, Chaus F, Fogg L, Dasgupta M, Straus D, Byrne RW. Learning curve for the transsphenoidal endoscopic endonasal approach to pituitary tumors. Br J Neurosurg 2016;30:637–42.
[38] Singh H, Essayed WI, Cohen-Gadol A, Zada G, Schwartz TH. Resection of pituitary tumors: endoscopic versus microscopic. J Neuro Oncol 2016;130:309–17.
[39] Snyderman C, Kassam A, Carrau R, Mintz A, Gardner P, Prevedello DM. Acquisition of surgical skills for endonasal skull base surgery: a training program. Laryngoscope 2007;117:699–705.
[40] Tandon A, Alzate J, LaSala P, Fried MP. Endoscopic endonasal transsphenoidal resection for pituitary apoplexy during the third trimester of pregnancy. Surg Res Pract 2014:397131.
[41] Wang AJ, Zaidi HA, Laws Jr ER. History of endonasal skull base surgery. J Neurosurg Sci 2016;60:441–53.
[42] Wang F, Zhou T, Wei S, Meng X, Zhang J, Hou Y, et al. Endoscopic endonasal transsphenoidal surgery of 1,166 pituitary adenomas. Surg Endosc 2015;29:1270–80.
[43] Zaidi HA, Zehri A, Smith TR, Nakaji P, Laws Jr ER. Efficacy of three-dimensional endoscopy for ventral skull base pathology: a systematic review of the literature. World Neurosurg 2016;86:419–31.